# DEM-based Convolutional Neural Network Modeling for Estimation of Solar Irradiation: Comparison of the Effect of DEM Resolutions

**J. Heo[a], J. Jung[a], B. Kim[b], and S. Han[a]**

[a]Dept. of Civil and Environmental Engineering, Hanyang University, Republic of Korea
[b]Dept. of Civil Engineering, Andong National University, Republic of Korea
E-mail: heojae1234@hanyang.ac.kr, jhjung1216@gmail.com, bkim@anu.ac.kr, sanguk@hanyang.ac.kr

**Abstract –**

**Recently, the use of solar panels has increased because of the growing demand for solar energy. To determine appropriate installation sites of photovoltaic (PV) panels, estimating the available solar energy at a certain area is important to predict the amount of power generation and planning PV plant operations. However, traditional data-driven approaches (e.g., machine learning) do not fully reflect the topographical characteristics of surrounding regions in the solar energy estimation, and the impact of data resolution (e.g., map scales) on the prediction accuracy has rarely been investigated. Thus, this paper presents a solar irradiation prediction model using a convolutional neural network (CNN) designed to process digital elevation map (DEM) images. Furthermore, an analysis of the impact of two different resolutions (i.e., 30 m and 60 m resolutions) on the model performance is also presented. A total of 25,000 DEM images are extracted from the national map of South Korea for both resolutions and then used as an input to train the CNN models. The results show that the CNN-based prediction models can be used to estimate the solar irradiation with high accuracy (e.g., mean square errors of 0.0018 and 0.0032 for 30 m and 60 m resolutions). It was also found that data resolution affects the performance of the CNN-based models. With an accurate estimation of the available solar energy at a certain site, the sites generating more power can potentially be evaluated and selected by searching a DEM on a large scale.**

**Keywords –**

**Solar energy, solar irradiation prediction, GIS, convolutional neural network**

## 1 Introduction

Global carbon dioxide emissions from fossil fuels, which are considered to be the major cause of global warming, have been constantly increasing in the last decade: for example, by an average of 3.1$\pm$0.2 GtC yr$^{-1}$ during 2008-2017 [1]. As global warming affects human health and causes the climate change, efforts such as environment regulation, emissions trading, clean energy technology development, and deforestation reduction have been made to control and reduce the pollution. An effective approach is replacing fossil fuel with renewable energy, such as solar energy, wind energy, biofuel energy, and so on. Particularly, the use of photovoltaics (PV) has rapidly grown, nearly quadrupling over the past five years [2]. Unlike other renewable energy sources, solar energy is considered to be economical: solar cells operate for a long period, generally more than 20 years, and require low maintenance expenses [3].

To meet the increasing demand for solar energy, the prediction of solar radiation that estimates the amount of available solar energy at a certain place is a key to planning the power supply [4]. Furthermore, the accurate estimation of available solar energy allows for the optimal selection of PV installation sites, as well as the decision on PV system [5, 6]. Although various approaches to the solar energy estimation (e.g., statistical model, fuzzy logic approaches, machine learning) have been proposed and used in practice, it is still challenging to collect solar radiation data on a large scale and consider the geographical characteristic of adjacent areas in the estimation. For example, solar radiation-related data that is used to estimate available solar energy is often collected from specific observation regions. Although this approach can be suitable for general terrain, it would be hard to assume that simple linear interpolation or any estimating method for topography measurements may work well for other regions far away from the observation stations or complex terrain (e.g., mountains) [7]. Furthermore, in general, statistical methods or conventional machine learning algorithms (e.g., Bayesian networks, support vector machines) do not directly process image or map type-data with the three-dimensional (3D) shape of an image (i.e., topography) [8]; while recent machine learning algorithms such as convolutional neural networks (CNN) are designed to keep spatial relationships among data points (e.g., pixels) in the modeling process (e.g., optimization of model parameters).

This research thus investigates the use of CNN for modeling and predicting the solar irradiation, taking into account the effect of geospatial features, including elevation, slope, aspect, shadow effect, and so on. Specifically, this paper mainly focuses on the impact of data resolutions on the prediction accuracy in order to understand the effect of map scale and geographical features on solar energy computation. The CNN model is trained with a digital elevation map (DEM) containing such topographical features and solar radiation datasets estimated in pixel levels. With the trained CNN model, performances for DEMs of 30 m and 60m resolutions are compared to evaluate the effect of data resolution.

# 2 Research Background

This section reviews recent studies that consider topographical features for predicting solar irradiation using machine learning techniques and statistical methods. In addition, the impact of data resolution on forecasting performance of solar irradiation is also reviewed and discussed.

## 2.1 Challenges in Solar Irradiation Prediction Considering the Topographical Features

Recent studies showed that the topographical features (e.g., altitude, latitude, longitude) considerably influenced the solar radiation prediction performance [7, 9, 10, 11]. For example, [7] estimated daily global solar irradiation by using solar radiation data collected on the complex mountainous terrain; it was found that the most important geographic factor to estimate global solar irradiation on complex mountainous terrain is the altitude. [9] developed the prediction model using solar radiation data observed in different regions in the model training and testing processes, showing that the solar radiation could successfully be estimated for new testing regions not used in the modeling process. Additionally, [10] evaluated geographical factors such as latitude, longitude, altitude in order to find the optimal combination of input parameters and to understand the impact of topographic features.

Overall, these previous studies provide insight into the use of data and the impact of topographical features on predicting solar irradiation by building statistical or machine learning models. Nonetheless, the models and methods proposed in the studies are mostly tested with the data collected at specific observation stations. This issue can become critical when applied to the regions far away from the study areas, where topographical characteristics can significantly be different. In this regard, further studies are still required for in-depth understanding of the topographical features in solar irradiation estimation, when the data-driven approaches are applied to large-scale areas or other areas, as pointed out in [11].

## 2.2 The Effect of Data Resolution on Solar Irradiation Prediction Model Performance

For machine learning or statistical methods, data resolution is another factor affecting the predicted amount of solar irradiation [12, 13]. The effect of data resolution was thus studied with a focus on the input data such as a DEM used to develop the geometry-based prediction model of solar radiation. In [12], geometry-based methods were developed using solar radiation models such as SRAD, Solei-32, and r.sun, which analyzed the components of solar radiation (e.g., direct, diffuse, and reflected) and geographic elements such as site latitude, topography, shadow cast, and so on. [12] found that the resolution change of a DEM affected the input variables of the prediction model, such as shadow effect, elevation, slope, etc., which resulted in a difference between the predicted solar radiation values and actual values. [13] also showed that a higher DEM resolution improved the performance of solar radiation models. These studies implied that the resolution of a DEM can affect the accuracy of surface angle calculations at the study area, which are the key inputs to theoretical computing of the solar radiation.

Unlike geometry-based methods, the impact of data resolution has rarely been studied for data-driven approaches that attempt to recognize patterns in the relevant data for the solar radiation prediction. It may be because machine learning methods in the previous studies [e.g., 14, 15] generally used solar radiation data (e.g., altitude, latitude, longitude, land surface temperature) produced at observation stations. In this case, the resolution of data may not be of importance for the prediction, as DEM data was not directly used for the modeling process. Consequently, the effect of data resolution still remains unknown when DEM data itself is used as an input for machine learning approaches to solar radiation estimation.

# 3 Method

To evaluate the effect of data resolution on machine learning-based solar energy prediction, this study builds and compares two CNN models trained with a DEM with 30m resolution and another DEM with 60 m resolution along with the average amount of solar radiation for each DEM map of 30 by 30 pixel. Specifically, the DEMs are created with GIS datasets publicly provided by the National Spatial Data Infrastructure (NSDI) in South Korea, and the DEM that covers the entire national territory with the grid cell size of 30 m by 30 m is selected to create the DEM datasets with different resolutions, i.e., the inputs for the CNN models. Meanwhile, the output datasets, which are the estimated solar irradiation in pixel levels (e.g., a raster with 30 m by 30 m), are obtained by applying the computational estimation model presented in the authors' prior work [16]. Then, with the datasets used as an input and an output, CNN models are built and trained through the processes that minimize errors between the actual and predicted outputs. Eventually, the errors between two models with different data resolutions are compared to evaluate the effect of topographical features on the prediction performance.

## 3.1 Data Collection

For supervised learning, adopted in this paper, input datasets and labeled output datasets are needed to develop the CNN-based prediction model by iteratively learning the model parameters (e.g., weights) from the datasets. In building a solar irradiation prediction model, the CNN architecture consists of an input layer of a DEM image and an output layer of a solar radiation value with hidden layers between the two. The solar radiation amount for the region on each DEM image is extracted from a solar radiation image—produced by [16]—corresponding to the DEM image. In addition, two types of DEM images with 30 m and 60 m resolutions are created to assess the effect of data resolution on solar irradiation prediction. Specifically, for the inputs, DEM images (Figure 1c) are created by converting the contour map (Figure 1a) composed of group of lines joining points of the same elevation, to a triangular irregular network (TIN) (Figure 1b), which are continuous triangular facets with an empty space between contour lines representing the elevation. The generated TIN is then converted to a DEM image in a raster format (Figure 1c), which stores the elevation value at each pixel. This DEM image is eventually used as the input dataset in the CNN model for solar irradiation prediction.

On the other hand, the outputs, solar radiation data is produced by applying the computational method [16] that can estimate solar radiation values at every pixel given a DEN image. In [16], to consider topographical characteristics, a theoretical solar radiation energy model is transformed into a solar radiation model with inclined surface (Equation 1), which consists of reflected radiation (Equation 2), diffuse radiation (Equation 3), and direct radiation (Equation 4). Here, β is the surface tilt angle, ρ is the surface reflectance, and $i$ is the incident angle. $I_{b,N}$, $I_{d,h}$ and $I_h$ derived from [17], which are used to estimate solar radiation for a sunny day, are the radiation per unit area, the scattering radiation in the horizontal plane, and the horizontal solar radiation, respectively. Notably, to calculate the surface tilt angle (β), a tilt angle map is generated from the DEM. Consequently, when the DEM resolution changes, the tilt angle (β), reflected radiation, diffuse radiation, and even solar radiation can also change together. By applying [16], annual solar radiation is obtained as a result, and used as output datasets for the CNN modeling of solar irradiation prediction.

$$I_c = I_{r,c} + I_{d,c} + I_{b,c} \tag{1}$$

$$I_{r,c} = \rho I_h \sin^2(\beta/2) \tag{2}$$

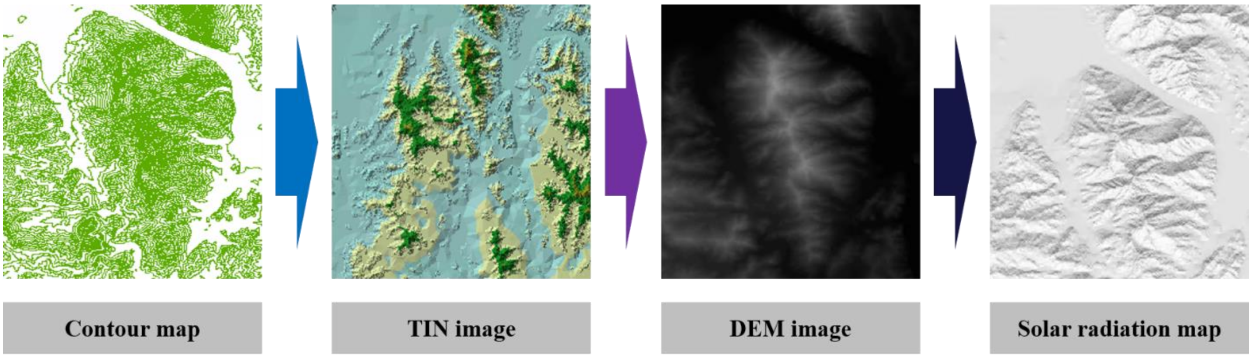


Figure 1. Overview of data collection and processing: (a) contour map, (b) TIN image, (c) DEM image, and (d) solar radiation map.

$$I_{d,c} = I_{d,h} \cos^2(\beta/2) \tag{3}$$

$$I_{b,c} = I_{b,N} \cos i \tag{4}$$

In addition, when generating the two datasets (i.e., for 30 m and 60 m resolutions), the geographic map resolution is determined by the horizontal and vertical length of one pixel (i.e., a raster), which represents the size of the region covered by the information (e.g., an elevation value) in one pixel. For example, the DEM with 30 m resolutions means that one pixel covers 900 $m^2$ area, and in this study, total 105,000 images are extracted and generated from the national map, while the DEM with 60 m resolution means that one pixel covers 3,600 $m^2$ area, and total 26,145 images are obtained from the national map. For the experiment comparing two data resolutions, 25,000 images are randomly selected from both datasets for the fairness of model comparison.

## 3.2 Data Modeling Approach

Deep learning, such as deep neural networks (DNN), is inspired by the human brain, imitating the vast human brain network with interconnected neurons. DNN is composed of an input layer that accepts external stimuli, hidden layers that act as mediators that allow each neuron to receive and to send signals, and an output layer that responds to signals from hidden layers [18]. These processes help to identify patterns and recognize features in an unordered dataset. However, traditional neural networks have a limitation in finding patterns or features in an image because of flattening three-dimensional image data to a single dimension in the learning process [8]. For example, three-dimensional DEM image containing elevation information in each pixel is transformed onto one-dimensional data, for example, a list shape in Figure 2a. In this case, spatial relationships among pixels are ignored in the learning process, and hence topographical patterns in DEM datasets are hardly learned in predicting the solar energy. However, CNN can utilize the DEM image as a three-dimensional input as it is, and the topographical features can still be learned in the modeling process. As DEM images pass through the convolutional layers, filters in the convolutional layers extract the features in DEM images, as shown in Figure 2b. Eventually, the model parameters (i.e., weights) in hidden layers are updated in iterations, in each of which a solar irradiation value is predicted using a regression function and compared to the actual value. Therefore, the CNN-based regression is adopted to solar irradiation given a DEM, taking into account the relationship between the topographical features and solar radiation.

## 3.3 CNN Architecture for Solar Irradiation Prediction

The architecture of the CNN-based regression is illustrated in Figure 3. The input layer is designed to receive an input image of 30 x 30 pixels, which represents a region of 900 m x 900 m for 30 m resolution data and 1,800 m x 1,800 m for 60 m resolution data. These input images (Figure 4) are extracted from the national map without any overlap, as described in Section 3.1.

The input image representing a DEM when entered to an input layer is then sent to the following convolution layer. The first convolution layer used to extract the feature maps of the DEM image is composed in 30 x 30 x 32 dimensions, which means a DEM window size of 30 x 30 pixels with 32 filters. The size of the filter used in this study is 3 x 3. The first convolution layer is connected to an activation function, a rectified linear unit (ReLU) function that controls and determines the output of the layer, which will be sent to the following layer, as well as to a max-pooling layer that helps reduce computation and overfitting by decreasing the size of input window. For instance, the input image (i.e., 30 x 30 pixels) is reduced to an image of 15 x 15 pixels through the max-pooling layer in the first convolution layer. The second and third layers (Figure 3) have similar structure to the first one, working similarly. The second convolution layer extracts the feature maps from the data of the previous layer by using the same number of filters as the one in the first layer. However, the third convolution layer uses the 64 filters to extract the feature maps, although the second and third convolution layers are also connected to the activation function layer and

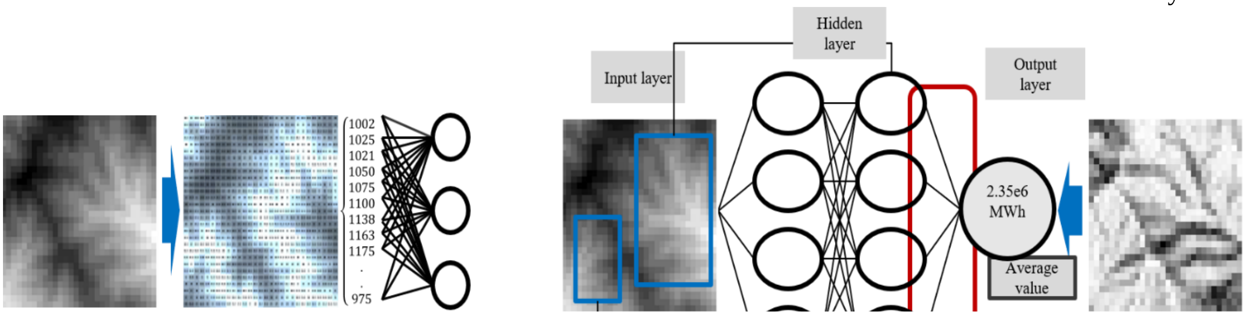


Figure 2. Overview of data modeling: (a) deep learning, and (b) convolutional neural network

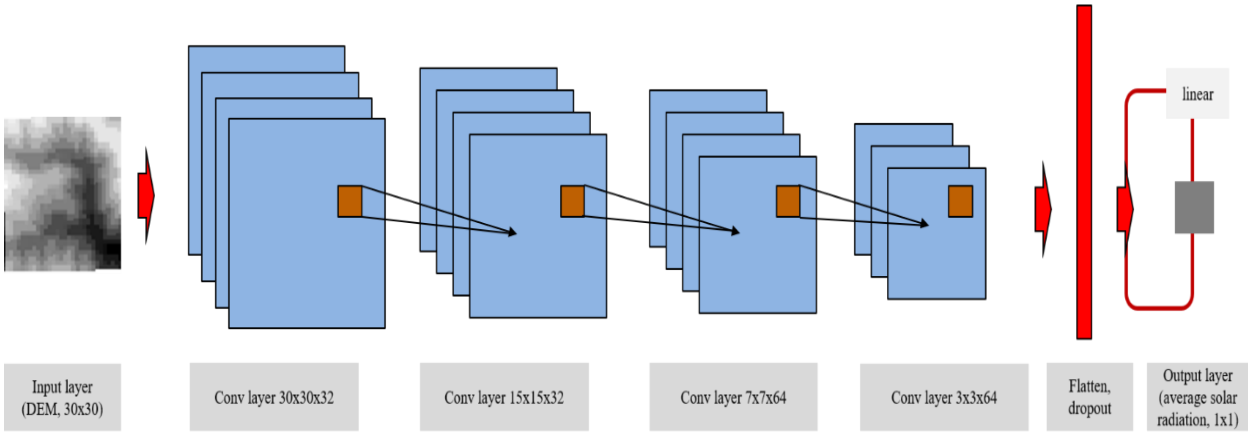


Figure 3. Architecture of convolutional neural network

max-pooling layer. The size of an input window thus decreased from 15 x 15 pixels to 7 x 7 pixels by passing the second max-pooling layer, and the size further decreased from 7 x 7 pixels to 3 x 3 pixels by passing the third max-pooling layer. The fourth layer is also a convolution layer with the same number of filters as the one in the third convolution layer, and the activation function layer; however, no max-pooling layer is included. The input data passed through the fourth layer is then sent to a dropout layer that is used to prevent the overfitting problem, and is in turn sent to a linear function layer for regression analysis (instead of a softmax function generally used for classification).

The CNN model described above is trained by using mean square error (MSE) as the loss function in the process that updates the model parameters (e.g., convolution filters) on the way that minimizes the error difference between the predicted value by the trained network and the actual solar radiation data. The MSE is defined in Equation 5, where $i$ denotes $i$-th data in the dataset, and $n$ is the number of training or testing samples in the dataset. The learning process of CNN continues in iterations until the minimum MSE, or the number of iterations a user defines, is reached. The resulting predicted value with a minimum error is compared with the actual one, and the coefficient of determination ($R^2$) is computed to evaluate the model performance. The value of the coefficient of determination is between 0 and 1; and for the higher correlation between the dependent variable and the independent variable, the value of coefficient of determination is closer to 1.

$$MSE = \frac{1}{n}\sum_{i=1}^{n}(actual - predicted)^2 \tag{5}$$

In this study, the MSEs and coefficient of determination are computed for the two CNN models built for the datasets with different data resolutions, to

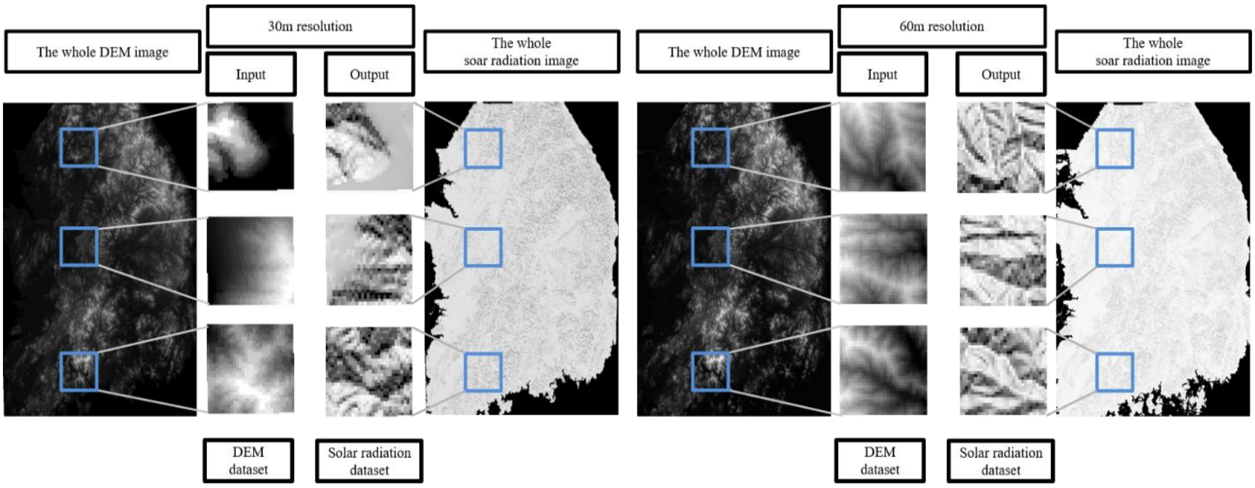


Figure 3. Overview of DEM and solar radiation datasets processing: (a) 30m resolution datasets and (b) 60m resolution datasets

assess the effect of data resolution on the solar irradiation prediction.

## 4 Experiment Results

Figure 4 illustrates a pair of two datasets: the DEM image and the corresponding solar radiation maps for two data resolutions. From the solar radiation map, annual mean of available solar irradiation is calculated for each map (i.e., 30 x 30 pixels), the mean value is used as an output the model attempts to predict. Particularly, the DEM image and solar radiation value are normalized as a pre-process. This normalization is adopted to prevent the poor learning caused by the wide spread of data values, and the min-max normalization method is applied for scaling the range of raw data to be [0, 1]. As a result, the raw DEM datasets for 30 m and 60 m resolutions (e.g., Figure 4a and 4b), the range of which are initially [0, 1900] and [0, 1550], respectively, are scaled to [0, 1]. The difference in the max values may happen for different DEM resolutions used to estimate the solar radiation. For example, higher-resolution data represents the elevation information more precisely than lower-resolution data [12]. This difference in data resolution affects the solar radiation data, the deviation of which between two resolutions is observed as approximately 11%.

Figures 5 and 6 present the relationship between the predicted and actual results for 30 m and 60 m resolutions, respectively. Overall, both results visually show that the predicted one is strongly correlated to the observed one with $R^2$ of 0.89 and 0.87.

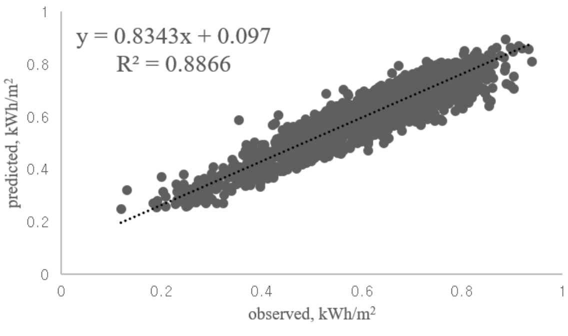


Figure 4. The plot of the relationship between the predicted and actual results for 30 m resolution

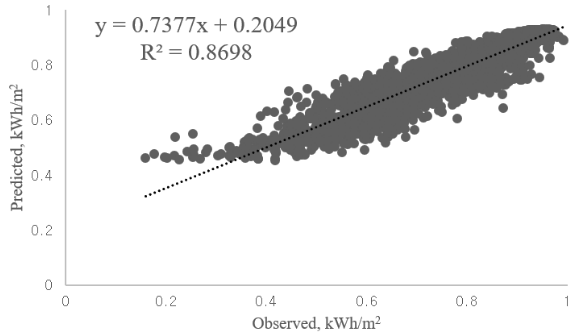


Figure 5. The plot of the relationship between the predicted and actual results for 60 m resolution

Table 1 summarizes the MSE, $R^2$, and MSE converted in actual units. The $R^2$ for 30 m resolution dataset is slightly higher than the one for 60 m resolution dataset. It is also observed that the plot of 30 m resolution (Figure 5) is slightly more uniformly distributed than the one of 60 m resolution (Figure 6). Yet, the difference caused by data resolution may not be significant in this experiment. Additionally, it is observed that the MSE value of 30 m resolution is 0.0018, while the MSE value of 60 m resolution is 0.00315. When converted in the actual units, the prediction errors of solar irradiation for 30 m and 60 m resolutions are 3,981 kWh/m$^2$ and 8,007 kWh/m$^2$, respectively. In other words, the errors from 30 m resolution data are 1.8 times and 2.0 times lower than the ones from 60 m resolution data in the MSE and MSE in actual unit, respectively. Thus, these results show that in this experiment, the solar irradiation is more accurately predicted when the data with higher resolution is used.

Table 1. Summary of the experiment results

| Data resolution | MSE | $R^2$ | MSE-in actual unit |
|---|---|---|---|
| 30 m | 0.0018 | 0.89 | 3,981 kWh/m$^2$ |
| 60 m | 0.0032 | 0.87 | 8,007 kWh/m$^2$ |

## 5 Discussion

In this paper, CNN-based prediction is adapted to reflect the topographical features in the solar energy estimation. The results indicate that the proposed CNN-based approach produces promising results for the prediction of the solar irradiation on complex terrains or on a large scale. The CNN model learns spatial correlations among individual pixel values stored in each image (e.g., an array) during the training, and thus it can be implied that the solar irradiation is fairly affected by the topography of a surrounding terrain. For example, the amount of solar irradiation on a surface can be significantly influenced by the shadow created by adjacent hills at high elevation. The proposed approach that can use a DEM image itself as an input thus enables us to utilize a map-type data for machine learning.

The results also reveal that, in this experiment, DEMs with higher resolution outperform ones with lower resolution when a machine learning method is applied. This result is also supported by [13], reporting that a higher DEM resolution produces more accurate results with geometry-based methods instead of machine learning applied in that study. This result may imply that when the topographical features are represented or preserved well in datasets, the solar irradiation can be better estimated, as the neural network is generally affected by the quality of image [19]. Thus, the resolution and quality of DEM inputs should be carefully selected and tested, depending on the level of accuracy required for the solar energy study.

Previous machine learning approaches have mainly focused on evaluating the geographical factors (e.g., altitude, latitude, longitude) as input variables or gathering the data related to solar energy from the meteorological observation sites. However, this study shows through the CNN modeling that geographical features can be reflected in the solar energy estimation model, and the effect of data resolution is also assessed for an CNN application. Nevertheless, there are other factors affecting the CNN performance, which should further be explored. For instance, the size of an image can have an impact on the CNN performance [20]. An input image of 30 x 30 pixel size is used in this study, but other image sizes (e.g., 60 x 60, 90 x 90) need to be studied for an in-depth understanding of the size of an area affecting the amount of solar radiation. On the other hand, the method of calculating the solar radiation used as output data can also affect the predictive performance. In this study, the mean of solar irradiations stored in a pixel level on a DEM image is used as an output the model estimates. As the solar radiation on the surface of the earth depends not only on the surface angle or the shape of the terrain but also on the position of the sun [21], specific regions with higher solar energy may exist. Thus, various regions representing the entire DEM image well (e.g., average, a top region, a middle region, top triangle shape on a DEM) should be tested to understand which part of a DEM can be better estimated with the DEM image.

## 6 Conclusion

This study investigates the effect of geographical features on a solar irradiation estimation model by using CNN models built based on the datasets with different data resolutions. The CNN uses DEM images in a 3D shape (e.g., an elevation value stored in x-y coordinates) as an input; thus, spatial information is still held and modelled during a learning process. Furthermore, it is found that the use of higher-resolution data can result in more accurate prediction in the experiment. Regardless of the data resolution; however, models for both resolutions produce robust estimation results (e.g., MSEs of 0.0018 and 0.0032). Thus, the CNN approach may allow for the appropriate selection of PV panel installation on a large scale. In our future study, the CNN model will be further developed to estimate the power generated at a PV panel site by investigating the CNN architecture for the use of multilayer inputs, including maps of weather conditions, which are other critical factors affecting the power generation.

## Acknowledgements

This research was supported by a grant (19CTAP-C141728-02) from Technology Advancement Research Program (TARP) funded by Ministry of Land, Infrastructure and Transport of Korean government.

## References

[1] Le Quéré. and Corinne. et al. Global carbon budget. *Earth System Science Data*, 10:2141-2194, 2018.
[2] BP Statistical Review of World Energy. On-line: http://bp.com, Accessed: 16/01/2019.
[3] Solar Power Advantages and Disadvantages: On-line: http://sepco-solarlighting.com, Accessed: 16/01/2019.
[4] Samanta. B. and Al Balushi. K. R. Estimation of incident radiation on a novel spherical solar collector. *Renewable energy*, 14(1-4):241-247, 1998.
[5] Escobedo and J. F. et al. Modeling hourly and daily fractions of UV, PAR, and NIR to global solar radiation under various sky conditions at Botucatu, Brazil. *Applied Energy*, 86(3):299-309, 2009.
[6] Faghih and A. K. et al. Solar radiation on domed roofs. *Energy and Buildings*, 41(11):1238-1245, 2009.
[7] Bosch. J. L and Lopez. G. et al. Daily solar irradiation estimation over a mountainous area using artificial neural networks. *Renewable Energy*, 33(7):1622-1628, 2008.
[8] Karpathy. A. Convolutional Neural Network for Visual Recognition. On-line: http://cs231n.github.io, Accessed: 17/01/2019.
[9] Mohandes. M and S. R. et al. Estimation of global solar radiation using artificial neural networks. *Renewable energy*, 14(1-4):179-184, 1998.
[10] Koca. A and Oztop. H. H. et al. Estimation of solar radiation using artificial neural networks with

different input parameters for Mediterranean region of Anatolia in Turkey. *Expert Systems with Applications*, 38(7):8756-8762, 2011.

[11] Linares-Rodriguez. A and Ruiz-Arias. J. A. et al. Generation of synthetic daily global solar radiation data based on ERA-Interim reanalysis and artificial neural networks. *Energy*, 36(8):5356-5365, 2011.

[12] Liu. M and Bárdossy. A. et al. GIS-based modeling of topography-induced solar radiation variability in complex terrain for data sparse region. *International Journal of Geographical Information Science*, 26(7):1281-1308, 2012.

[13] Ruiz-Arias and J. A. et al. A comparative analysis of DEM-based models to estimate the solar radiation in mountainous terrain. *International journal of Geographical Information Science*, 23(8):1049-1076, 2009.

[14] Şahin. M and Kaya. Y. et al. Application of extreme learning machine for estimating solar radiation from satellite data. *International Journal of Energy Research*, 38(2):205-212, 2014.

[15] Şenkal. O. Solar radiation and precipitable water modelling for Turkey using artificial neural networks. *Meteorology and Atmospheric Physics*, 127(4):481-488, 2015.

[16] Jung. J and Han. S. et al. Digital Numerical Map-Oriented Estimation of Solar Energy Potential for Site Selection of Photovoltaic Solar Panels on National Highway Slopes. *Applied Energy*, 2019.

[17] Gueymard and C. A. Direct and indirect uncertainties in the prediction of tilted irradiance for solar engineering applications. *Solar Energy*, 83(3):432-444, 2009.

[18] Zaccone. G and Karim. M, R. et al. Deep learning with TensorFlow. volume 302(13). Packt, Livery Place 35 Livery Street Birmingham B3 2PB UK, 2017.

[19] Dodge. S and Karam. L. Understanding how image quality affect deep neural networks. In *Proc. Of QoMEX*, pages 1-6, Portugal, 2016.

[20] Howard and Andrew. G. Some improvements on deep convolutional neural network based image classification. On-line: https://arxiv.org/abs/1312-.5402/, Accessed 01/26/2019.

[21] Dubayah. R and Rich. P. M. Topographic solar radiation models for GIS. *International Journal of Geographical Information Systems*, 9(4):405-419, 1995.